Cluster States from Gaussian States: Essential Diagnostic Tools for Continuous-Variable One-Way Quantum Computing

Carlos González-Arciniegas,[1,*] Paulo Nussenzveig,[2] Marcelo Martinelli,[2] and Olivier Pfister[1]

[1] *Department of Physics, University of Virginia, 382 McCormick Road, Charlottesville, Virginia 22904-4714, USA*

[2] *Instituto de Física, Universidade de São Paulo, São Paulo, 05315-970, Brazil*

(Received 13 December 2019; revised 22 July 2021; accepted 9 August 2021; published 13 September 2021)

Continuous-variable (CV) cluster states are a universal quantum computing platform that has experimentally outscaled qubit platforms by orders of magnitude. Room-temperature implementation of CV cluster states has been achieved with quantum optics by using multimode squeezed Gaussian states. It has also been proven that fault tolerance thresholds for CV quantum computing can be reached at realistic squeezing levels. In this paper, we show that standard approaches to design and characterize CV cluster states can miss entanglement present in the system. Such hidden entanglement may be used to increase the power of a quantum computer but it can also, if undetected, hinder the successful implementation of a quantum algorithm. By a detailed analysis of the structure of Gaussian states, we derive an algorithm that reveals hidden entanglement in an arbitrary Gaussian state and optimizes its use for one-way quantum computing.

DOI: 10.1103/PRXQuantum.2.030343

I. INTRODUCTION

Continuous-variable (CV) quantum information [1–3] has achieved groundbreaking scalability performance [4–9] in the universal, measurement-based, one-way quantum computing (QC) model [10]. The CVQC model uses Gaussian (in terms of their Wigner function) cluster states as mathematical substrates [11] together with required non-Gaussian resources (such as photon counting measurement or a cubic phase gate) to constitute a universal quantum computation platform [10,12–15]. The idealized CVQC model uses, in lieu of qubits, spectrally dense qumodes such as the respective eigenstates $\{|s\rangle_q\}_{s\in\mathbb{R}}$ and $\{|s\rangle_p\}_{s\in\mathbb{R}}$ of the amplitude-quadrature operator $Q=(a+a^\dagger)/\sqrt{2}$ and phase-quadrature operator $P=i(a^\dagger-a)/\sqrt{2}$ of the quantized electromagnetic field, a being the photon annihilation operator. These quadrature eigenstates are infinitely squeezed states, which require infinite energy and are therefore unphysical. Realistic CVQC uses qumodes in squeezed Gaussian states, generated by SU(1,1) quadratic Hamiltonians. Such states are arbitrarily good approximations to quadrature eigenstates and also allow a fault tolerance threshold for amounts of squeezing of 10–20 dB [16–18] that are experimentally reachable [19].

Such reasonably high fault-tolerant squeezing levels may lead to the false impression that the analysis of the corresponding states would be essentially equivalent to their analysis in the infinite squeezing limit. This is incorrect. We show in this paper that the infinite squeezing limit fails to capture a subtle but crucial property of Gaussian states, which we call "hidden entanglement." We show that hidden entanglement can disrupt quantum computing if unaccounted for in a CV cluster state. However, hidden entanglement can always be detected and can sometimes be corrected.

To frame the problem in the most general way, we use the graphical calculus formalism developed by Menicucci *et al.* [20], whose gist is that any pure multimode Gaussian state can be described by a unique graph whose vertices denote the qumodes and whose complex-weighted edges denote the interactions between the qumodes sharing an edge. In this formalism, the real parts of the edge weights denote controlled-phase interactions, which are the CV analogs of controlled-Z gates for qubits [21]. These real edges therefore define the graph of a CV cluster state [11] that is usable for measurement-based, universal quantum computing [10,22,23].

It had been assumed that if Gaussian local unitaries (GLUs [24]; which cannot change the entanglement of the state) are applied to make the imaginary edge weights of the graph vanishingly small (e.g., in the limit of infinite squeezing), then a valid cluster state is obtained.

*cag2ze@virginia.edu

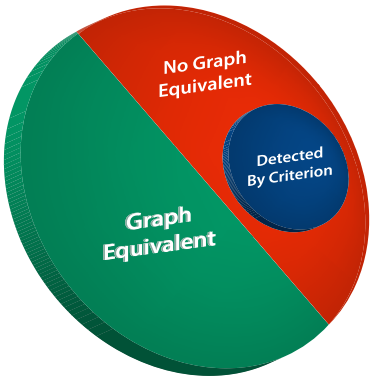

FIG. 1. Venn diagram of all Gaussian states. The two subsets are states that can (green) or cannot (red) be cast as a CV cluster state. Some of the invalid graph states are detectable by our sufficient criterion (blue subset). If applied to the whole set, our analytic procedure to express a Gaussian state as a graph state will succeed for the whole green subset.

In this paper, we show that the above procedure is not unique: starting from a given Gaussian state, there are different choices of GLUs that all give a vanishingly small imaginary graph but do give real graphs that have dramatically different entanglement, for example, containing or not containing disconnected subgraphs (i.e., seemingly separable quantum states). If the vanishingly small imaginary graph is ignored, this creates the paradoxical and unacceptable situation of the same state being GLU-equivalent both to separable states and to completely inseparable states.

This paradox is resolved by realizing that the entanglement that seems to disappear from the real graph under a GLU becomes "hidden" by being transferred to the imaginary graph. We must therefore ensure that the GLU leads to an imaginary graph that has no edge between two different qumodes.

We report two mathematical results: (i) we derive a sufficient mathematical criterion to find Gaussian states that have uncorrectable (i.e., "irreducible") hidden entanglement, which means that not all their imaginary edges can be transferred to real ones under any GLU and that these states cannot be expressed as cluster states; (ii) we derive an analytic algorithm to express a Gaussian state into a valid CV cluster state (i.e., with *null* imaginary edge weights). This algorithm is applicable to any Gaussian state and succeeds for all valid CV cluster states. The whole situation is summarized in Fig. 1.

These results enable us to answer the long-standing question of whether every Gaussian state can be expressed as a cluster state: the answer is negative.

This paper is structured as follows. In Sec. II, we pose the problem of identifying Gaussian states that cannot be expressed as valid cluster states. In Sec. III, we derive a sufficient criterion, (i) above, to identify Gaussian states that are not equivalent to cluster states. In Sec. IV, we derive a general algorithm, (ii) above, for expressing a Gaussian state as a valid cluster state. In the final section, we summarize our conclusions and discuss their relevance for quantum information science.

II. THE PROBLEM: ARE ALL GAUSSIAN STATES VALID CV CLUSTER STATES?

A. Introduction to the CV cluster state formalism

1. Qubits

A cluster state $|\psi_V\rangle$ [25] is a graph quantum state [26] that contains all the entanglement ever needed for any quantum algorithm [27] and that must be sparsely connected to be useful for quantum computing [28–30]. In the qubit paradigm, a graph state is composed of qubit vertices in the $|+\rangle = (|0\rangle + |1\rangle)/\sqrt{2}$ state, linked by controlled-Z gate edges. Quantum computation proceeds from a cluster state solely by single-qubit measurements and feedforward to graph neighbors. An N-qubit graph state can be defined as a stabilizer state (i.e., a simultaneous eigenstate of the N generators of the stabilizer group with eigenvalue 1). These generators are defined as

$$K_j = \hat{\sigma}_x^{(j)} \prod_{k=1}^{N} \left(\hat{\sigma}_z^{(k)}\right)^{V_{jk}}, \quad j = 1, 2, \ldots, N, \tag{1}$$

$$K_j |\psi_V\rangle = |\psi_V\rangle, \qquad j = 1, 2, \ldots n, \tag{2}$$

where the V_{jk} denote the elements of the adjacency matrix $\mathbf{V}$ of the graph: V_{jk}=1 if there is an edge between qubits j and k and V_{jk}=0 otherwise. The operators $\hat{\sigma}_{x,z}^{(j)}$ are Pauli operators acting on qubit j.

2. Qumodes

An ideal CV graph state $|\Psi_V\rangle$ is constructed by preparing each qumode vertex in a zero-phase eigenstate $|0\rangle_p = \int |s\rangle_q \, ds/\sqrt{2\pi}$ and then applying controlled phase displacements as per the adjacency matrix $\prod_{j\geq k}^{N} \exp(i\mathbf{V}_{jk} Q_j Q_k)$ [10,11]. The generators of the stabilizer group are of the form $K_j = e^{i\alpha \mathcal{N}_j}$, $\alpha \in \mathbb{R}$, with $\mathcal{N}_j$ denoting the nullifier operators [22]

$$\mathcal{N}_j = P_j - \sum_{k=1}^{N} V_{jk} Q_k, \quad j = 1, 2, \ldots n, \tag{3}$$

$$\mathcal{N}_j |\Psi_V\rangle = 0 |\Psi_V\rangle, \qquad j = 1, 2, \ldots n, \tag{4}$$

where $\mathbf{V}$ is now a weighted adjacency matrix, whose elements can have any real value. These ideal CV states are infinitely squeezed and therefore unphysical.

3. Finitely squeezed states

In the laboratory, one uses the closest approximations to quadrature eigenstates, which are Gaussian phase-quadrature-squeezed vacuum states

$$|\,0,r\,\rangle \propto \int dq\; e^{-\frac{1}{2}e^{-2r}q^2}\;|\,q\,\rangle \propto \int dp\; e^{-\frac{1}{2}e^{2r}p^2}\;|\,p\,\rangle\,, \quad (5)$$

where $r > 0$ is the squeezing parameter and coincides with the logarithmic gain of a parametric amplifier such as an optical parametric oscillator below threshold. A valid Gaussian approximation of an ideal graph state $|\Psi_V\rangle$ of adjacency matrix $\mathbf{V}$ must then fulfill the property

$$\mathrm{cov}\,[\mathbf{P}-\mathbf{V}\mathbf{Q}] \xrightarrow[r\to\infty]{} \mathbb{0}, \quad (6)$$

where $\mathrm{cov}[\mathbf{A}]_{jk} = (1/2)\,\langle\Psi_V|\,\{A_j, A_k\}\,|\Psi_V\rangle$ is an element of the covariance matrix of operator vector $\mathbf{A}=(A_1,\ldots,A_n)^T$.

It was shown by Menicucci *et al.* [20] that the effects of finite squeezing can be fully taken into account by defining a complex graph $\mathbf{Z} = \mathbf{V} + i\mathbf{U}$, where $\mathbf{V}$ is the weighted symmetric adjacency matrix as before and $\mathbf{U}$ is a symmetric positive definite matrix that accounts for all finite squeezing effects [31]. Any pure Gaussian state $|\,\Psi_Z\,\rangle$ [32] can be written in the position representation as

$$\langle\,\mathbf{q}\,|\,\Psi_Z\,\rangle = \Psi_Z(\mathbf{q}) = \pi^{-N/4}\,(\det\mathbf{U})^{1/4}\exp\left(\frac{i}{2}\mathbf{q}^T\mathbf{Z}\mathbf{q}\right), \quad (7)$$

the positive definiteness of $\mathbf{U}$ ensuring that the state is normalizable. The complex matrix $\mathbf{Z}$ defines exact graph state nullifiers

$$(\mathbf{P}-\mathbf{Z}\mathbf{Q})\,|\,\Psi_Z\,\rangle = \mathbf{0}\,|\,\Psi_Z\,\rangle\,. \quad (8)$$

These nullifiers are non-Hermitian operators and therefore not suited for measurement-based quantum computation. Nonetheless, we can still use the nullifiers given by the adjacency matrix $\mathbf{V}$ if we realize that the wave function of Eq. (7) satisfies the relation

$$\mathrm{cov}\,[\mathbf{P}-\mathbf{V}\mathbf{Q}] = \frac{1}{2}\mathbf{U}, \quad (9)$$

and note that, as long as $\mathbf{U}\to\mathbb{0}$ or, equivalently, $\mathrm{Tr}[\mathrm{U}]\to 0$ given that $\mathbf{U}$ is positive definite, we recover Eq. (6). It has been proposed that having a vanishingly small $\mathbf{U}$ is enough to claim that our Gaussian state approximates an ideal graph state with adjacency matrix $\mathbf{V}$ and, hence, we could think of $\mathbf{U}$ (or $\mathrm{Tr}[\mathrm{U}]$) as the error on approximating an ideal CV graph state [20]. Note from Eqs. (6) and (9) that $\mathbf{U}=\mathbb{0}$ is logically equivalent to the infinite squeezing limit.

If $\mathrm{Tr}[\mathbf{U}]$ is vanishingly small, we may be tempted to completely disregard $\mathbf{U}$ and think of $\mathbf{Z}$ as the ideal graph $\mathbf{Z}=\mathbf{V}$. This has been, until now, the main way to deal with Gaussian graph states but, as we show next using the covariance matrix, this definition alone may ignore strong quantum correlations present in the system, which can lead to large errors in the characterization of its entanglement, as we show in Sec. II B 1.

4. Covariance matrix

A Gaussian state is fully characterized by its covariance matrix. The quadrature-ordered covariance matrix is

$$\mathbf{\Sigma}^{(\mathrm{quad})} = \mathrm{cov}[\mathbf{R}] = \begin{pmatrix}\mathrm{cov}[\mathbf{Q}] & \mathrm{cov}[\mathbf{Q},\mathbf{P}]\\ \mathrm{cov}[\mathbf{P},\mathbf{Q}] & \mathrm{cov}[\mathbf{P}]\end{pmatrix} \quad (10)$$

$$\mathbf{\Sigma}^{(\mathrm{quad})} = \frac{1}{2}\begin{pmatrix}\mathbf{U}^{-1} & \mathbf{U}^{-1}\mathbf{V}\\ \mathbf{V}\mathbf{U}^{-1} & \mathbf{U}+\mathbf{V}\mathbf{U}^{-1}\mathbf{V}\end{pmatrix}, \quad (11)$$

where $\mathbf{R} = (\mathbf{Q},\mathbf{P})^T$. Examination of the upper-left block in Eqs. (10) and (11) yields the formula

$$\mathrm{cov}\,[\mathbf{Q}] = \frac{1}{2}\mathbf{U}^{-1} \quad (12)$$

and a first observation: *the off-diagonal entries of* $\boldsymbol{U}^{-1}$ may be large, describing strong quantum correlations that could still appear vanishingly small in $\mathbf{U}$ and therefore be missed. We must therefore supplement the $\mathrm{Tr}[\mathrm{U}]\to 0$ criterion [Eq. (9)] for finitely squeezed Gaussian states [20] by also requiring that $\mathbf{U}^{-1}$ be diagonal, which is logically equivalent to $\mathbf{U}$ being diagonal [33]. This will ensure that all the correlations of the system are encoded exclusively in the adjacency matrix $\mathbf{V}$.

Before addressing the diagonalization of $\mathbf{U}$ in detail, we first give two concrete examples of hidden entanglement.

B. Examples of hidden entanglement

1. Two qumodes

We consider here the very simple case of two independent single-mode squeezed states, of respective parameters r_1 and r_2, interfering at a balanced beam splitter. Derivation details can be found in Appendix A. The resulting graph is purely imaginary:

$|\,\mathcal{B}(0,r_1,r_2)\,\rangle_{12} =$ 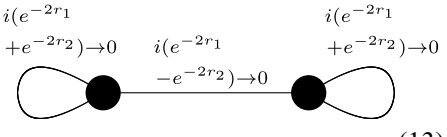

(13)

Since all edges are exponentially decreasing with the squeezing, a logical conclusion would be that the state is,

for all intents and purposes, equivalent to the product state obtained in the infinite squeezing limit, i.e.,

$$|\,\mathcal{B}(0,r_1,r_2)\,\rangle_{12} \underset{r_{1,2}\to\infty}{\longrightarrow}$$  (14)

This conclusion is incorrect. While state $|\,\mathcal{B}(0,r,r)\,\rangle_{12}$ is, indeed, an exact product state (which was demonstrated experimentally [34]), state $|\,\mathcal{B}(0,r_1,r_2\neq r_1)\,\rangle_{12}$ can, however, be strongly entangled. We now prove this.

An independent quantitative bipartite entanglement criterion is the generalization of the Peres-Horodecki partial transpose criterion [35,36] to continuous variables [37] (see also Ref. [38]). Bipartite CV nonseparability is characterized by the symplectic eigenvalues of the covariance matrix $\tilde{\mathbf{\Sigma}}$ of the partially transposed density operator, which is equivalent to a phase space reflection [37]: if the original covariance matrix is $\mathbf{\Sigma}$, then $\tilde{\mathbf{\Sigma}}=\mathbf{\Lambda}\mathbf{\Sigma}\mathbf{\Lambda}$, where $\mathbf{\Lambda}$=diag$(1,1,-1,1)$. Entanglement is present if at least one of the symplectic eigenvalues of $\tilde{\mathbf{\Sigma}}$ is less than $1/2$, their product being $1/4$. These symplectic eigenvalues are defined as the absolute values of the eigenvalues of $i\tilde{\mathbf{\Sigma}}\mathbf{\Omega}$, with $\mathbf{\Omega}=\left(\begin{smallmatrix}0 & \mathbb{1}\\ -\mathbb{1} & 0\end{smallmatrix}\right)$. The symplectic eigenvalues of $|\,\mathcal{B}(0,r_1,r_2)\,\rangle_{12}$ are

$$\lambda_{\pm}=\tfrac{1}{2}\,e^{\pm(r_1-r_2)}, \tag{15}$$

which shows that the state is a product state if and only if $r_1=r_2$ but can be significantly entangled if the difference r_1-r_2 is large. Let us take the case $r_1=2r_2$ with r_2 already large (e.g., 20- and 10-dB squeezing). Then the amount of entanglement in $|\,\mathcal{B}(0,2.30,1.65)\,\rangle_{12}$ is equivalent to that present in a 10-dB-squeezed two-mode squeezed state, even though all edges in Eq. (13) are vanishing.

Thus, the null graph edges given by $\mathbf{V}$ clearly fail to give the proper description here, even though Tr[U] $\to 0$ in both cases. The key points are that the infinite squeezing limit incorrectly symmetrizes the situation, giving the wrong description for finite squeezing, and that the vanishingly small, *yet nonzero* off-diagonal entries of $\mathbf{U}$ still yield large $\langle Q_iQ_j\rangle$ correlations from $\mathbf{U}^{-1}$, as per Eq. (11), which are key to the discrepancy.

If we use single-mode symplectic transformations (i.e., GLUs) to diagonalize $\mathbf{U}$, the entanglement cannot be changed [37,39]. We therefore seek GLUs that transform $|\,\mathcal{B}(0,r_1,r_2\neq r_1)\,\rangle_{12}$ into a two-mode squeezed state of equal entanglement: the result is (Appendix A)

$$|\,\mathcal{E}\,(r_-)\,\rangle_{12}=S_1\,(r_+)\,S_2\,(r_+)|\,\mathcal{B}(0,r_1,r_2)\,\rangle_{12}\,, \tag{16}$$

where $S(r)=\exp[(r/2)(a^{\dagger 2}-a^2)]$ is a phase squeezing operator (for $r>0$) and $r_\pm=(r_1\pm r_2)/2$. Equation (16) solves the conundrum: in finitely squeezed states, entanglement can be hidden by single-mode squeezing in nonsymmetric cases, where the squeezing is not evenly distributed between the modes. This situation is always absent in the infinitely squeezed case, which is, by force, totally symmetric.

After single-mode squeezing operations, Eq. (16), and phase shifts carry out $\mathbf{Z}\mapsto\mathbf{Z}'$, we obtain [see Eq. (A18)]

$$\mathrm{Tr}[\mathbf{U}']=2\mathrm{sech}(r_1-r_2)\underset{r_1>r_2\gg 1}{\longrightarrow}4e^{-(r_1-r_2)}, \tag{17}$$

which can be compared with the value of Eq. (13), before the single-mode squeezing operations,

$$\mathrm{Tr}[\mathbf{U}]=2(e^{-2r_1}+e^{-2r_2})\underset{r_1>r_2\gg 1}{\longrightarrow}2e^{-2r_2}. \tag{18}$$

While both traces tend to zero in the infinite squeezing limit, graph $\mathbf{V}'$ [Eq. (A19) with $r=r_-$] reveals the entanglement of the state, whereas graph $\mathbf{V}$ [Eqs. (13) and (14)] does not.

Another important instance of quantum state distortion invisible in the infinite squeezing limit is the generation of a two-mode squeezed state from the interference of orthogonal single-mode squeezed states,

$$\left|\,\mathcal{B}(\tfrac{\pi}{2},r,r)\,\right\rangle=|\,\mathcal{E}(r)\,\rangle\,, \tag{19}$$

which is relevant to a multitude of CV quantum information experiments, a few prominent examples of which are given in Refs. [6–9,40,41]. If the states are not identically squeezed, we get

$$\left|\,\mathcal{B}(\tfrac{\pi}{2},r_1,r_2)\,\right\rangle=S_1(-r_-)S_2(-r_-)\,|\,\mathcal{E}(r_+)\,\rangle\,, \tag{20}$$

which features, on top of the desired two-mode squeezing by r_+, excess uncorrelated quantum noise on each qumode, each being independently antisqueezed by r_-.

2. Six qumodes

We now turn to a highly multipartite example and show that the two dramatically different graphs in Fig. 2 are GLU-equivalent.

The top part of Fig. 2 represents the real part (adjacency matrix $\mathbf{V}$) of the six-mode graph $\mathbf{Z}=\mathbf{V}+i\mathbf{U}$:

$$\mathbf{V}=\begin{pmatrix}0&0&t&0&0&0\\0&0&t&0&0&0\\t&t&0&0&0&0\\0&0&0&0&0&0\\0&0&0&0&0&t\\0&0&0&0&t&0\end{pmatrix}, \tag{21}$$

$$\mathbf{U}=\begin{pmatrix}c^{-1}&0&0&0&0&0\\0&c^{-1}&0&0&0&0\\0&0&c^{-1}&-c^{-1}t&c^{-1}t^2&0\\0&0&-c^{-1}t&c^{-1}&-c^{-1}t&0\\0&0&c^{-1}t^2&-c^{-1}t&c^{-1}&0\\0&0&0&0&0&c^{-1}\end{pmatrix}, \tag{22}$$

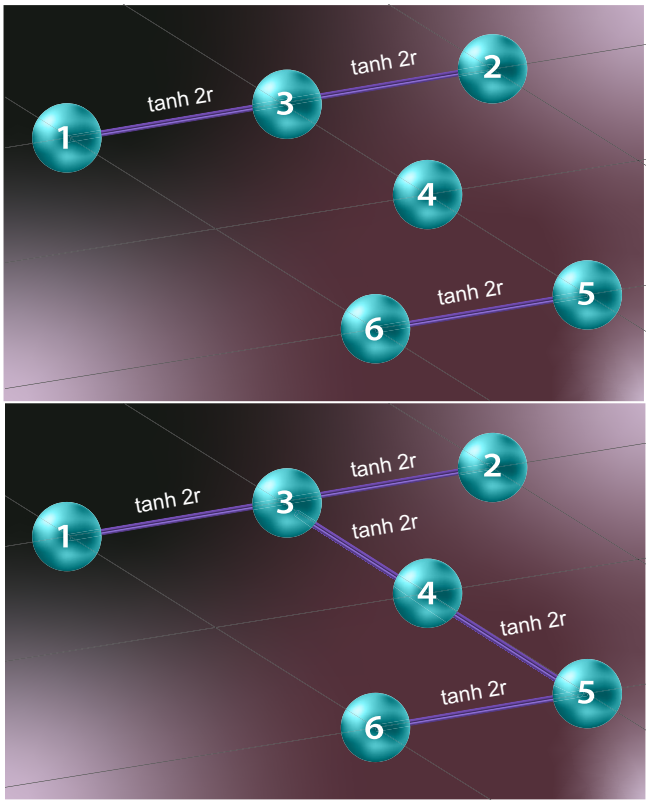

FIG. 2. Top: Cluster state graph given by matrix **V** in Eq. (21). Note the three disconnected subgraphs. Bottom: Cluster state graph given by matrix **V'** in Eq. (29), obtained by diagonalizing **U**′ by GLUs. The state is now one connected graph, all hidden entanglement having been revealed.

where $t = \tanh 2r$ and $c^{-1} = \operatorname{sech} 2r$. This state clearly verifies $\mathbf{U} \to \mathbf{0}$ for $r \to \infty$, because $t \to 1$ and $c^{-1} \to 0$. The top part of Fig. 2 shows three disconnected graphs, the chain 1-3-2, the chain 5-6, and sole qumode 4. The top part of Fig. 2, however, is incorrect: there are hidden quantum correlations, or hidden entanglement, between modes 3, 4, and 5, which are present in **U** and will disrupt quantum computation over the cluster state. For example, a measurement of isolated qumode 4 is not expected to affect the rest of the graph since it is disconnected from it. Yet it will. These hidden correlations can actually be quite strong, even with Tr[U] $\to$ 0. We can see this from Eq. (12). In this instance we have

$$\mathbf{U}^{-1} = \begin{pmatrix} c & 0 & 0 & 0 & 0 & 0 \\ 0 & c & 0 & 0 & 0 & 0 \\ 0 & 0 & c^3 & s\,c^2 & 0 & 0 \\ 0 & 0 & s\,c^2 & c(c^2+s^2) & s\,c^2 & 0 \\ 0 & 0 & 0 & s\,c^2 & c^3 & 0 \\ 0 & 0 & 0 & 0 & 0 & c \end{pmatrix}, \tag{23}$$

where $c = \cosh 2r$ and $s = \sinh 2r$, which are very large. The only way to suppress these spurious correlations is, of course, to diagonalize **U**. This must be done without changing the entanglement of the graph state (i.e., using only local symplectic, equivalently local linear unitary, operations, i.e., GLUs). In this work, we identify all situations where this is feasible and demonstrate a GLU-diagonalization procedure that will succeed whenever possible. In that sense, given any Gaussian state, we are now able to ascertain whether it is a valid cluster state (i.e., with **U** diagonal and Tr[U] $\to$ 0) or not.

Let us go back to our six-mode example. A Gaussian unitary $\mathcal{U}$ can be represented in the Heisenberg picture by a symplectic matrix **S** such that

$$\mathbf{R}' = \mathcal{U}^\dagger \mathbf{R} \mathcal{U} = \mathbf{S}\mathbf{R}. \tag{24}$$

The symplectic symmetry requires that **S** fulfill $\mathbf{S}\boldsymbol{\Omega}\mathbf{S}^T = \boldsymbol{\Omega}$, which is equivalent to preserving the canonical commutation relations $[R_j, R_k] = [R'_j, R'_k] = \Omega_{jk}$. Any GLU must then have the form

$$\mathcal{U} = \bigotimes_{j=1}^{N} \mathcal{U}_j, \tag{25}$$

$$\mathbf{S} = \bigoplus_{j=1}^{N} \mathbf{S}_j \tag{26}$$

so that

$$\begin{pmatrix} Q'_j \\ P'_j \end{pmatrix} = \mathcal{U}_j^\dagger \begin{pmatrix} Q_j \\ P_j \end{pmatrix} \mathcal{U}_j = \mathbf{S}_j \begin{pmatrix} Q_j \\ P_j \end{pmatrix} \quad j = 1, \ldots, N. \tag{27}$$

In our example, taking **U** to a diagonal from can be done with single-mode squeezing GLUs:

$$\mathbf{S}_1 = \mathbf{S}_2 = \mathbf{S}_3^{-1} = \mathbf{F}\mathbf{S}_4^{-1} = \mathbf{S}_5^{-1} = \mathbf{S}_6 = \begin{pmatrix} c^{-1} & 0 \\ 0 & c \end{pmatrix}, \tag{28}$$

where $\mathbf{F} = \left(\begin{smallmatrix} 0 & -1 \\ 1 & 0 \end{smallmatrix}\right)$ is a $\pi/2$ rotation in phase space (also known as a Fourier transform). Under this transformation the **Z** graph becomes $\mathbf{Z}' = \mathbf{V}' + i\mathbf{U}'$, with [20]

$$\mathbf{V}' = \begin{pmatrix} 0 & 0 & t & 0 & 0 & 0 \\ 0 & 0 & t & 0 & 0 & 0 \\ t & t & 0 & t & 0 & 0 \\ 0 & 0 & t & 0 & t & 0 \\ 0 & 0 & 0 & t & 0 & t \\ 0 & 0 & 0 & 0 & t & 0 \end{pmatrix}, \tag{29}$$

$$\mathbf{U}' = \begin{pmatrix} c^{-3} & 0 & 0 & 0 & 0 & 0 \\ 0 & c^{-3} & 0 & 0 & 0 & 0 \\ 0 & 0 & c^{-1} & 0 & 0 & 0 \\ 0 & 0 & 0 & c^{-1} & 0 & 0 \\ 0 & 0 & 0 & 0 & c^{-1} & 0 \\ 0 & 0 & 0 & 0 & 0 & c^{-3} \end{pmatrix}. \tag{30}$$

Now that **U**′ is diagonal (still with Tr[**U'**] $\to$ 0), no hidden entanglement is present and the **V**′ graph at the bottom

of Fig. 2 shows the complete picture, which includes the expected 3-4 and 4-5 entanglement edges.

As we mentioned earlier, the previous best practice for calculating the closest graph **V'** approximated by a given Gaussian state, minimizing Tr[**U**] solely by local rotations [20], does not suffice here. As we have shown in these two examples, one must strive to make **U** diagonal by using all possible GLUs, including squeezing and shearing.

Finally, it is important to realize that this procedure does not always succeed: there are cases where hidden entanglement is irreducible and cannot be transferred to **V** under GLUs (i.e., where there exist no GLUs that can make **U** diagonal). We now examine these cases.

III. SUFFICIENT CRITERION FOR DETECTING IRREDUCIBLE HIDDEN ENTANGLEMENT

In this section, we address the question of detecting irreducible hidden entanglement (i.e., the Gaussian states whose matrix **U** *cannot* be diagonalized by GLUs). Such states consequently cannot be made GLU-equivalent to a CV cluster state.

If **U** is diagonal, we can write, from Eq. (12),

$$\mathrm{cov}[\mathbf{Q}] = \mathrm{diag}\{\lambda_1, \lambda_2, \ldots, \lambda_N\}, \tag{31}$$

where $\lambda_j > 0, j = 1, 2, \ldots, N$. This yields

$$2\langle Q_j Q_k\rangle = \lambda_j \delta_{jk}, \tag{32}$$

$$\langle\{Q_j, P_k\}\rangle = \lambda_j V_{jk}, \tag{33}$$

$$2\langle P_j P_k\rangle = \lambda_j^{-1}\delta_{jk} + \sum_l V_{jl}\lambda_l V_{lk}. \tag{34}$$

We now use the more convenient mode-ordered covariance matrix, defining $\mathbf{x} = (Q_1, P_1, Q_2, P_2, \ldots, Q_N, P_N)^T$,

$$\mathbf{\Sigma}^{(\mathrm{mode})} = \mathrm{cov}[\mathbf{x}] = \begin{pmatrix} \boldsymbol{\sigma}_{11} & \boldsymbol{\sigma}_{12} & \cdots & \boldsymbol{\sigma}_{1n} \\ \boldsymbol{\sigma}_{21} & \boldsymbol{\sigma}_{22} & \cdots & \boldsymbol{\sigma}_{2n} \\ \vdots & \vdots & \ddots & \vdots \\ \boldsymbol{\sigma}_{n1} & \boldsymbol{\sigma}_{n2} & \cdots & \boldsymbol{\sigma}_{nn} \end{pmatrix}, \tag{35}$$

where

$$\boldsymbol{\sigma}_{jk} = \frac{1}{2}\begin{pmatrix} \langle\{Q_j, Q_k\}\rangle & \langle\{Q_j, P_k\}\rangle \\ \langle\{P_j, Q_k\}\rangle & \langle\{P_j, P_k\}\rangle \end{pmatrix} = \frac{1}{2}\begin{pmatrix} (\mathbf{U}^{-1})_{jk} & (\mathbf{U}^{-1}\mathbf{V})_{jk} \\ (\mathbf{V}\mathbf{U}^{-1})_{jk} & (\mathbf{U} + \mathbf{V}\mathbf{U}^{-1}\mathbf{V})_{jk} \end{pmatrix}, \tag{36}$$

which means that σ_{jj} is the covariance matrix of qumode j and $\sigma_{j\neq k} = \sigma_{k\neq j}^T$ contains all correlations between qumodes j and k. In this ordering, the direct-sum GLU of Eq. (26) can be written in block-diagonal form:

$$\mathbf{S}_{\mathrm{local}} = \begin{pmatrix} \mathbf{S}_1 & \mathbb{0} & \cdots & \mathbb{0} \\ \mathbb{0} & \ddots & \ddots & \vdots \\ \vdots & \ddots & \ddots & \mathbb{0} \\ \mathbb{0} & \cdots & \mathbb{0} & \mathbf{S}_N \end{pmatrix}. \tag{37}$$

Under GLUs, the covariance matrix blocks evolve as

$$\boldsymbol{\sigma}_{jk} \mapsto \boldsymbol{\sigma}'_{jk} = \mathbf{S}_j \boldsymbol{\sigma}_{jk} \mathbf{S}_k^T. \tag{38}$$

This allows us to establish a first important theorem.

Theorem. *The determinant of the correlation matrix σ_{jk}, $\det[\sigma_{jk}]$ is invariant under GLUs.*

Proof. This follows from the fact that the determinant of any symplectic matrix **S** is det[**S**]=1. Then, Eq. (38) yields $\det[\sigma'_{jk}]=\det[\sigma_{jk}]$. ■

The next theorem provides a sufficient, although not necessary, criterion for whether a given Gaussian state is not GLU-equivalent to a cluster state.

Theorem. *If a given Gaussian state is GLU-equivalent to a graph state, then* $\det[\sigma_{jk}] \leqslant 0$ *for all* $(j, k \neq j)$.

Proof. Let us go back to the **U** diagonal case. Using Eqs. (31)–(34), we can write

$$\boldsymbol{\sigma}_{jj} = \begin{pmatrix} \lambda_j & 0 \\ 0 & \mathrm{cov}[\mathbf{P}]_{jj} \end{pmatrix}, \tag{39}$$

$$\boldsymbol{\sigma}_{j\neq k} = \begin{pmatrix} 0 & \lambda_j V_{jk} \\ \lambda_k V_{jk} & \mathrm{cov}[\mathbf{P}]_{jk} \end{pmatrix}, \tag{40}$$

where we have assumed, without loss of generality, that we do not have any self-loops on our real graph, i.e., $V_{jj} = 0$ for all j [42]. From Eq. (40), we deduce that the determinant of $\sigma_{jk}, j \neq k$, for **U** diagonal is

$$\det[\sigma_{jk}] = -\lambda_j \lambda_k V_{jk}^2 \leqslant 0. \tag{41}$$

Note that $\det[\sigma_{jk}]=0 \Leftrightarrow V_{jk}=0$. Since $\det[\sigma_{jk}]$ is GLU-invariant, any Gaussian state that is GLU-equivalent to a cluster state (i.e., has **U** diagonal) has nonpositive $\det[\sigma_{jk}]$ for all $j \neq k$. ■

The theorem is not a logical equivalence because there are more submatrices σ_{jk} to process than available GLUs when $N(N-1)/2 > N$ (i.e., when the total number of qumodes $N > 3$). In this case, it is possible to have states with $\det[\sigma_{jk}] \leqslant 0$ for all $(j, k \neq j)$ that are nonetheless not GLU-equivalent to a cluster state.

Exceptions to this are the cases $N = 2$, for which all two-mode pure states are GLU-equivalent to two-mode squeezed states and also to two-mode cluster states, and $N = 3$, for which the number of submatrices σ_{jk} is $N(N-1)/2 = 3$ and three-mode Gaussian states with $\det[\sigma_{jk}] \leqslant 0$ for all $(j, k \neq j)$ are therefore GLU-equivalent to cluster states (see Appendix B).

The contraposition of the theorem above yields the sufficient criterion for Gaussian states that cannot be expressed as graph states, because $\mathbf{U}$ cannot be diagonalized by GLUs:

If there exists $(j, k \neq j)$ *such that* $\det[\sigma_{jk}] > 0$*, then the corresponding Gaussian state is not GLU-equivalent to a graph state.*

To use this criterion, one just has to check all off-diagonal 2×2 minors of the mode-ordered covariance matrix: a single positive $\det[\sigma_{jk}]$ is proof that irremovable hidden entanglement exists between j and k and that the corresponding state can never be GLU-equivalent to a cluster state.

IV. GENERAL ALGORITHM FOR DIAGONALIZING U BY GAUSSIAN LOCAL UNITARIES

We now extend the analysis of the previous section to deriving a general algorithm for diagonalizing $\mathbf{U}$ using GLUs.

The algorithm is based on noticing, from the quadrature-ordered covariance matrix of Eqs. (10) and (11), that the complete absence of amplitude correlations, $\langle Q_j Q_k \rangle = 0$ for all j and k, is logically equivalent to a diagonal $\mathbf{U}^{-1}$ and hence to a diagonal $\mathbf{U}$. We now introduce the GLU aspect of the diagonalization algorithm, which is best seen in the mode-ordered covariance matrix of Eqs. (35)–(36): we require a set of GLUs that cancel the upper-left entry of all 2×2 submatrices σ_{jk}. Because there are up to $N(N-1)/2$ such submatrices and only N available GLUs, it is clear that the algorithm cannot always be successful: for $N > 3$, canceling multiple $\langle Q_j Q_k \rangle$ with a single GLU will be required, thereby placing symmetry constraints on the Gaussian state under consideration. A detailed study of such constraints is outside the scope of this paper.

One should note that the algorithm will succeed for all Gaussian states that are GLU-equivalent to cluster states (green subset in Fig. 1) and will fail for all the rest (red subset in Fig. 1), including those undetected by the sufficient criterion derived in Sec. III.

We first proceed to define a "standard" covariance matrix of a valid Gaussian graph state (i.e., for which $\mathbf{U}$ is diagonal). We draw inspiration from the definition of a standard covariance matrix for LU-equivalent Gaussian states by Adesso [39] and Giedke and Kraus [43]. We first define the single-mode squeezing operations

$$\mathbf{T}_j = \begin{pmatrix} \lambda_j^{-1/2} & 0 \\ 0 & \lambda_j^{1/2} \end{pmatrix}, \quad j = 1, \ldots, N. \tag{42}$$

Then, using the transformation rule of Eq. (38), we define the standard covariance matrix as

$$\tilde{\boldsymbol{\sigma}}_{jj} = \mathbf{T}_j \boldsymbol{\sigma}_{jj} \mathbf{T}_j^T = \begin{pmatrix} 1 & 0 \\ 0 & \lambda_j \operatorname{cov}[\mathbf{P}]_{jj} \end{pmatrix}, \tag{43}$$

$$\tilde{\boldsymbol{\sigma}}_{j \neq k} = \mathbf{T}_j \boldsymbol{\sigma}_{jk} \mathbf{T}_k^T = \sqrt{\lambda_j \lambda_k} \begin{pmatrix} 0 & V_{jk} \\ V_{jk} & \operatorname{cov}[\mathbf{P}]_{jk} \end{pmatrix}, \tag{44}$$

where the off-diagonal terms of $\tilde{\boldsymbol{\sigma}}_{jk}$ are the same and equal to $\pm\sqrt{-\det[\boldsymbol{\sigma}_{jk}]}$. It is easy to see that this form corresponds to a diagonal $\mathbf{U}$ by virtue of Eq. (36).

The goal is to find N single-mode GLUs that take all covariance submatrices

$$\sigma_{j \neq k} = \begin{pmatrix} a_{jk} & b_{jk} \\ c_{jk} & d_{jk} \end{pmatrix} \tag{45}$$

to the standard form of Eq. (44). Each of the N sought GLUs is written as an Iwasawa decomposition [[44–46]]:

$$\mathbf{S}_j = \begin{pmatrix} 1 & 0 \\ q_j & 1 \end{pmatrix} \begin{pmatrix} r_j & 0 \\ 0 & r_j^{-1} \end{pmatrix} \begin{pmatrix} \cos\phi_j & -\sin\phi_j \\ \sin\phi_j & \cos\phi_j \end{pmatrix}, \tag{46}$$

where $r_j > 0$. The leftmost matrix in Eq. (46) corresponds to a shearing transformation that shifts the diagonal elements of $\mathbf{V}$: $V_{jj} \mapsto V_{jj} + q_j$. This does not play any role in the process of diagonalizing $\mathbf{U}$, so without loss of generality we can set $q_j = 0$, allowing us to reduce the number of free parameters of $\mathbf{S}_j$ to only two. The second matrix, where $r_j > 0$, corresponds to a single-mode squeezing and the third matrix corresponds to a single-mode rotation. To find GLUs that diagonalize $\mathbf{U}$, we proceed by sequentially finding the parameters r_j and ϕ_j in Eq. (46) by operating one by one in all the correlation submatrices $\sigma_{j \neq k}$ and taking them to the standard form of Eq. (44). It is important to point out that two GLUs $\mathbf{S}_j$ and $\mathbf{S}_k$ act simultaneously on each given $\sigma_{j \neq k}$, as shown by Eq. (38); hence, at each stage of the process of eliminating the term $\langle Q_j Q_k \rangle$, both GLUs $\mathbf{S}_j$ and $\mathbf{S}_k$ must be taken into account at the same time. This procedure varies slightly depending on whether $\det[\sigma_{j,k}] < 0$, as presented below, or $\det[\sigma_{j,k}] = 0$, as presented in Appendix C.

Assuming that $\det[\sigma_{j,k}] \neq 0$, let $\mathbf{M} = \left(\begin{smallmatrix} A & B \\ C & D \end{smallmatrix}\right)$ be a general 2×2 matrix. If we want to use the GLU multiplying to the

left in Eq. (38), we find a GLU $\mathbf{S}_{\text{left}}$ such that

$$\mathbf{S}_{\text{left}}\mathbf{M} = \begin{pmatrix} 0 & \delta \\ \delta & \delta\,\frac{AB+CD}{A^2+C^2} \end{pmatrix}, \tag{47}$$

where $\delta = \sqrt{-\det[\mathbf{M}]} = \sqrt{BC - AD}$. The Iwasawa parameters are

$$\cos\phi_{\text{left}} = \frac{C}{\sqrt{A^2+C^2}}, \quad \sin\phi_{\text{left}} = \frac{A}{\sqrt{A^2+C^2}}, \tag{48}$$

$$r_{\text{left}} = \delta^{-1}\sqrt{A^2+C^2}. \tag{49}$$

Likewise, we can use a GLU to the right:

$$\mathbf{M}\mathbf{S}_{\text{right}}^{T} = \begin{pmatrix} 0 & \delta \\ \delta & \delta\,\frac{AC+BD}{A^2+B^2} \end{pmatrix}, \tag{50}$$

with

$$\cos\phi_{\text{right}} = \frac{B}{\sqrt{A^2+B^2}}, \quad \sin\phi_{\text{right}} = \frac{A}{\sqrt{A^2+B^2}}, \tag{51}$$

$$r_{\text{right}} = \delta^{-1}\sqrt{A^2+B^2}. \tag{52}$$

If we set $\mathbf{M} = \sigma_{jk}\mathbf{S}_k^T$ in Eqs. (47) and (48), then we have taken σ_{jk} to the standard form using only $\mathbf{S}_j$ regardless of the value that $\mathbf{S}_k$ may take. If $\mathbf{S}_k$ was already determined in a previous stage, then Eq. (48) fixes the value of $\mathbf{S}_j$. On the other hand, if the $\mathbf{S}_k$ have not been determined yet, then we will have that $\mathbf{S}_j$ will be a function of $\mathbf{S}_k$ (and σ_{jk}), denoted as $\mathbf{S}_j\,[\mathbf{S}_k]$, and $\mathbf{S}_k$ can be used to take another submatrix σ_{kl}, $l \neq j$, to the standard form. Using other matrices σ_{mj}, $m \neq k$ and taking them to the standard form via the procedure above, we can find expressions of the form $\mathbf{S}_m = \mathbf{S}_m\left[\mathbf{S}_j\right] = \mathbf{S}_m\,[\mathbf{S}_k]$ (where we have taken into account that $\mathbf{S}_j = \mathbf{S}_j\,[\mathbf{S}_k]$). Finally the value of $\mathbf{S}_k$ can be found using a correlation matrix of type σ_{km}, where the α'_{km} term must cancel out from the equation $\boldsymbol{\sigma}'_{km} = \mathbf{S}_k\boldsymbol{\sigma}_{km}\mathbf{S}_m[\mathbf{S}_k]^T$. Explicit forms of $\mathbf{S}_j\,[\mathbf{S}_k]$, more details of this procedure, and how it is modified when we have singular matrices can be found in Appendix C.

The algorithm is complete when all the N GLUs are determined using the above procedure, which, in general, makes use of a subset of all the correlation matrices σ_{jk}. As shown in Appendix C, the case may present itself where we find multiple solutions for the GLUs $\mathbf{S}_j, j = 1,\ldots,N$, but those solutions are the most general ones that take the correlation submatrices σ_{jk} used through the algorithm to the standard form. Therefore, the last step is to apply those solutions to the remaining correlation matrices that were not used yet and test whether they all also take the standard form. If one of these GLU sets successfully zeroes out all $\langle Q_j Q_k\rangle$ terms, for all j and $k, j \neq k$, then the corresponding Gaussian state is a valid (GLU-equivalent) CV cluster state, otherwise there exists irreducible hidden entanglement.

V. CONCLUSION

We have reported and fully analyzed a fundamental effect that is specific of continuous-variable quantum information and does not occur in qubit-based quantum information. This effect is linked to the description of any Gaussian Wigner function, in the Iwasawa decomposition, by a complex graph state [20] whose stabilizers are not necessarily unitary or, equivalently, whose nullifiers are not necessarily Hermitian. For the graph to provide a valid representation of a cluster state—with unitary stabilizers and Hermitian nullifiers—the imaginary part of the graph must vanish. Whereas all previous work ensured that this always occurred in the infinite squeezing limit, our work shows that this limit is not reliable as state asymmetries can give rise to hidden entanglement, at times irreducibly so. Such hidden entanglement may morph into a more versatile and useful cluster state but will disrupt quantum information processing if not accounted for. An interesting extension of this work might be to explore its possible connections to an earlier study of tripartite entanglement by Adesso and Illuminati [47], in which pure, symmetric three-mode Gaussian states were shown to be simultaneous CV analogs of both the Greenberger-Horne-Zeilinger state and the the W state of three qubits.

A simple occurrence of this effect is present in the case of the workhorse of entanglement generation: the interference of two orthogonally squeezed quantum quadratures at a balanced beam splitter [40], which will exhibit excess quantum noise, as per Eq. (20), if the initial squeezed modes have different parameters. This is a heretofore undiscovered source of imperfections in realistic CV quantum information experiments. This result emphasizes the importance of forgoing the use of the infinite squeezing limit as more than a simplification when dealing with continuous-variable quantum information. An example of this philosophy is a recent result on the fault tolerance of statistical mixtures of cluster states in CVQC [18].

We emphasize here that our results do not alter the feasibility of continuous-variable quantum computing with finitely squeezed Gaussian states. Indeed, it is well known that these Gaussian resources must be completed by non-Gaussian ones, necessary for exponential speedup [14, 15] and fault tolerance [16]. Moreover, one should also remember that the resilience of cluster states under measurement [25] makes it straightforward to cut out of a Gaussian complex graph its irreducibly imaginary edges (if they are reasonably local) so as to make the graph real and therefore a valid CV cluster state.

Our work constitutes the first concrete analytic correspondence between arbitrary Gaussian states and CV cluster states. This paves the way to deriving mappings between cluster states and the universal Bloch-Messiah decomposition of Gaussian states [48], which opens up a new area of research of translating nonconventional

quantum circuits, such as Gaussian boson sampling [49], into cluster states and one-way quantum computing.

This work is also relevant to quantum state engineering given that it allows us to identify when a given general scalable source of entangled Gaussian states can be also a source of CV cluster states, which are a platform for universal quantum computation.

ACKNOWLEDGMENTS

We thank Nicolas Menicucci, Rafael Alexander, and Israel Klich for stimulating discussions. We are grateful to one of the referees for pointing out the work of Ref. [47]. This work was supported by NSF grant PHY-1820882, by the College of Arts and Sciences of the University of Virginia, by FAPESP SPRINT grant 2016/50468-7, and by Jefferson Lab LDRD project no. LDRD21-17 under which Jefferson Science Associates LLC manages and operates Jefferson Lab.

APPENDIX A: HIDDEN ENTANGLEMENT AND DIAGONALIZATION OF U BY GLUs IN THE TWO-MODE CASE

An ideal two-mode cluster state is defined as two $p = 0$ momentum eigenstates coupled by a $CZ = \exp(iQ_1Q_2)$ gate

$$|\mathcal{C}\rangle_{12} = \quad \mathrm{C_Z} = e^{iQ_1Q_2} \tag{A1}$$

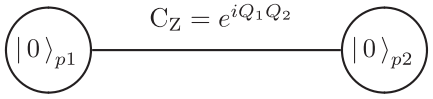

which admit the following nullifiers:

$$(\mathbf{P} - \mathbf{V}\mathbf{Q})\,|\mathcal{C}\rangle_{12} = \mathbf{0}\,|\mathcal{C}\rangle_{12}\,, \tag{A2}$$

where $\mathbf{Q}$=$(Q_1,Q_2)^T$, $\mathbf{P}$=$(P_1,P_2)^T$, and $\mathbf{V} = \left(\begin{smallmatrix} 0 & 1 \\ 1 & 0 \end{smallmatrix}\right)$.

In this appendix we study how different finitely squeezed two-mode states relate to this ideal cluster state as we approach the infinite squeezing limit.

We focus on the simple but fundamental case of the state created by the interference at a balanced beam splitter of two quadrature eigenstates out of phase by θ:

$$|\mathcal{B}(\theta)\rangle_{12} = B_{12}\,|0\rangle_{\theta 1}\,|0\rangle_{p2}\,, \tag{A3}$$

where $B_{12} = \exp[-i(\pi/4)(a_1^\dagger a_2 + a_1 a_2^\dagger)]$ and where the generalized-quadrature nullifier and eigenstate are

$$A_1(\theta)\,|0\rangle_{\theta 1} = (\cos\theta\, P_1 + \sin\theta\, Q_1)\,|0\rangle_{\theta 1} = 0\,|0\rangle_{\theta 1}\,. \tag{A4}$$

The nullifiers of $|\mathcal{B}(\theta)\rangle_{12}$ are

$$\mathcal{N}_1 = B_{12}P_2B_{12}^\dagger = P_1 - P_2, \tag{A5}$$

$$\mathcal{N}_2(\theta) = B_{12}A_1(\theta)B_{12}^\dagger = \sin\theta\,(Q_1 + Q_2) + \cos\theta\,(P_1 + P_2). \tag{A6}$$

For $\theta = 0$, these nullifiers are $P_1 \pm P_2$. As the stabilizers form a multiplicative group, the nullifiers form an additive one and a linear combination of nullifiers is a nullifier. Hence, P_1 and P_2 nullify $|\mathcal{B}(0)\rangle_{12}$, which entails $\mathbf{V} = \mathbb{0}$:

$$|\mathcal{B}(0)\rangle_{12} = |0\rangle_{p1}\,|0\rangle_{p2} = \tag{A7}$$

An edge between two vertices signifies entanglement, its absence signifies separability, and GLUs cannot transform two separated subgraphs into a connected one.

For $\theta = \pi/2$, we recover the nullifiers of the Einstein-Podolsky-Rosen state [50]

$$(Q_1 - Q_2)\,|\mathcal{E}\rangle_{12} = 0\,|\mathcal{E}\rangle_{12}\,, \tag{A8}$$

$$(P_1 + P_2)\,|\mathcal{E}\rangle_{12} = 0\,|\mathcal{E}\rangle_{12}\,, \tag{A9}$$

which entails

$$\left|\mathcal{B}\left(\tfrac{\pi}{2}\right)\right\rangle_{12} = |\mathcal{E}\rangle_{12} \overset{\mathrm{GLU}}{\sim} |\mathcal{C}\rangle_{12}\,. \tag{A10}$$

For $\theta < \pi/2$, we can rewrite the nullifiers of Eqs. (A5) and (A6) in cluster state form,

$$\mathbf{V} = \frac{1}{2}\begin{pmatrix} \tan\theta & \tan\theta \\ \tan\theta & \tan\theta \end{pmatrix}, \tag{A11}$$

which corresponds to the graph

$$|\mathcal{B}(\theta)\rangle_{12} = \tag{A12}$$

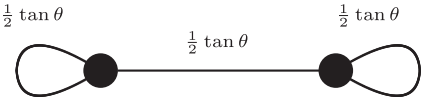

State $|\mathcal{B}(\theta)\rangle_{12}$ is therefore GLU-equivalent to a cluster state, as expected since all bipartite entangled states are equivalent under GLUs.

We now turn to the generalization to Gaussian states of the graphical formalism introduced above, which was developed by Menicucci *et al.* [20]. The gist of this formalism is that any pure Gaussian state can be represented by a unique graph whose edges are weighted by *complex* numbers, the imaginary edges representing the effect of the squeezing. This is because the nullifier of a phase-squeezed state of finite squeezing parameter r is not P anymore but is $P - i\,e^{-2r}Q$. As a result, the adjacency matrix $\mathbf{Z}$ of the graph becomes complex:

$$\mathbf{Z} = \mathbf{V} + i\mathbf{U}, \tag{A13}$$

where $\mathbf{V}$ is as before. Matrix $\mathbf{U}$ is symmetric, like $\mathbf{V}$, and also positive definite. It represents the effects of finite

squeezing [20] and can be interpreted as the error of the Gaussian state in approximating an ideal graph state of weighted adjacency matrix $\mathbf{V}$, as per

$$\mathrm{cov}[\mathbf{P}-\mathbf{V}\mathbf{Q}]=\frac{1}{2}\mathbf{U}, \tag{A14}$$

which generalizes Eq. (A2), cov denoting the covariance matrix of the nullifiers. Hence, a Gaussian state $\mathbf{Z}$ is a good approximation of a graph state $\mathbf{V}$ if $\mathbf{U}\to\mathbb{0}$, or $\mathrm{Tr}[\mathrm{U}]\to 0$ since $\mathbf{U}$ is positive definite.

The canonical Gaussian cluster state has two phase-squeezed qumodes [realistic implementations of phase-quadrature eigenstates, i.e., finite squeezing version of Eq. (A1)], of respective squeezing parameters r_1 and r_2, linked by controlled-phase gates:

$$\mathbf{Z}_{\mathcal{C}}\equiv\begin{pmatrix}0&1\\1&0\end{pmatrix}+i\begin{pmatrix}e^{-2r_1}&0\\0&e^{-2r_2}\end{pmatrix}, \tag{A15}$$

$|\,\mathcal{C}(r_1,r_2)\,\rangle_{12}=$ 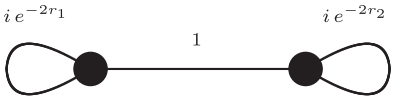

(A16)

Our next example is the Gaussian Einstein-Podolsky-Rosen state, also known as the two-mode squeezed state $|\,\mathcal{E}(r)\,\rangle_{12}$, where r is the squeezing parameter [40]. Solving the Heisenberg equations for the two-mode squeezing Hamiltonian $i(r/\tau)a_1^\dagger a_2^\dagger+$ H.c. over time τ, one finds [51]

$$\Delta\,(Q_1-Q_2)=\Delta\,(P_1+P_2)=e^{-r}, \tag{A17}$$

which coincides with the nullifiers of Eqs. (A8) and (A9) in the infinite squeezing limit $r\to\infty$. Using Gaussian graphical calculus, we find, after a $(\pi/2)$ rotation of one mode [20],

$$\mathbf{Z}_{\mathcal{E}}\equiv\begin{pmatrix}0&\tanh 2r\\\tanh 2r&0\end{pmatrix}+i\begin{pmatrix}\mathrm{sech}\,2r&0\\0&\mathrm{sech}\,2r\end{pmatrix}, \tag{A18}$$

$\mathcal{F}_1\,|\,\mathcal{E}(r)\,\rangle_{12}=$ 

(A19)

In the limit $r\to\infty$ and up to a GLU (here a Fourier transform), Eqs. (A16) and (A19) are identical.

The next case is much less trivial. The finitely squeezed version of $|\,\mathcal{B}(\theta)\,\rangle_{12}$, Eq. (A3), is

$$|\,\mathcal{B}(\theta,r_1,r_2)\,\rangle_{12}=B_{12}R_1(\theta)S_1(r_1)S_2(r_2)\,|\,0\,\rangle_1\,|\,0\,\rangle_2\,, \tag{A20}$$

where the initial state is a vacuum, $S(r)=\exp[(r/2)(a^{\dagger 2}-a^2)]$ is a phase squeezing operator for $r>0$, and $R(\theta)=\exp(-i\theta a^\dagger a)$ is a phase-space rotation operator. The Gaussian graph is

$$\mathbf{Z}\equiv v\begin{pmatrix}1&1\\1&1\end{pmatrix}+i\begin{pmatrix}u_+&u_-\\u_-&u_+\end{pmatrix}, \tag{A21}$$

$|\,\mathcal{B}(\theta,r_1,r_2)\,\rangle_{12}=$ 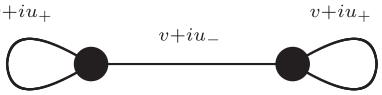

(A22)

where

$$v=-\frac{\sin 2\theta\,\sinh 2r_1}{2(e^{2r_1}\cos^2\theta+e^{-2r_1}\sin^2\theta)}, \tag{A23}$$

$$u_\pm=\frac{e^{-2r_1}}{\cos^2\theta+e^{-4r_1}\sin^2\theta}\pm e^{-2r_2}. \tag{A24}$$

In an initial analysis of this situation for $0<\theta<\pi/2$, one is tempted to dismiss $\mathbf{U}$ altogether as its elements $u_\pm$ clearly decrease as the squeezing factors decrease. Turning then to $\mathbf{V}$, entanglement is clearly present since $v\neq 0$. This result is well known [52].

For $\theta=(\pi/2)$, we know the result must be a two-mode squeezed state [41]. However, we have

$$v=0, \tag{A25}$$

$$u_\pm=e^{2r_1}\pm e^{-2r_2}. \tag{A26}$$

Entanglement would appear to have vanished ($\mathbf{V}=\mathbb{0}$) but here the effects of finite squeezing cannot be ignored any longer: the diverging $\mathbf{U}$ makes $\mathbf{V}$ irrelevant as an approximation of a graph state by a Gaussian state. It was proposed in Ref. [20] that the closest CV graph state that can be approximated by a given Gaussian state could be found by minimizing the trace of $\mathbf{U}$ by local rotations. An extremum of $\mathrm{Tr}[\mathrm{U}]$ can always be reached using $\pi/2$ qumode rotations, i.e., Fourier transforms [53]. This property yields

$$\mathbf{U'}=\begin{pmatrix}e^{r_1-r_2}\mathrm{sech}(r_1+r_2)&0\\0&e^{r_2-r_1}\mathrm{sech}(r_1+r_2)\end{pmatrix}, \tag{A27}$$

$$\mathbf{V'}=\begin{pmatrix}0&\tanh(r_1+r_2)\\\tanh(r_1+r_2)&0\end{pmatrix}, \tag{A28}$$

$\mathcal{F}\,|\,\mathcal{B}(\frac{\pi}{2},r_1,r_2)\,\rangle_{12}=$ 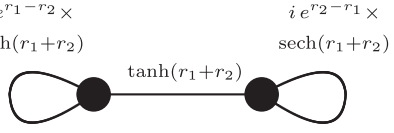

(A29)

which yields Eq. (A19) for $r_1=r_2=r$ and Eq. (A1) for $r\to\infty$.

APPENDIX B: THREE-MODE CASE

In this section we show that for the case of three modes, the requirement $\det\{\sigma_{jk}\} < 0$ is not only necessary but also sufficient for a state to be GLU to a diagonal **U** state. The concept of standard forms of covariance matrices was developed in Refs. [[39,43]], where two Gaussian states are GLU-equivalent if and only if they have the same standard form of their covariance matrices.

The process to calculate the standard form is to decompose each local operation in its Bloch-Messiah decomposition $\mathbf{S}_j = \mathbf{M}_j \mathbf{\Lambda}_j \mathbf{N}_j^T$, where $\mathbf{N}_j$ and $\mathbf{M}_j$ are rotation matrices and $\mathbf{\Lambda}_j$ is a diagonal squeezing matrix. $\mathbf{M}_j$ and $\mathbf{\Lambda}_j$ are then used to symplectically diagonalize all the σ_{jj} (i.e., make them proportional to the identity). Finally, after applying these first two operations, we use $\mathbf{N}_j$ to diagonalize as many σ_{jk}, matrices as possible ($j \neq k$). To do this, we use the singular value decomposition $\sigma_{jk} = \mathbf{A}_{jk}\mathbf{D}_{jk}\mathbf{B}_{jk}$, where $\mathbf{A}_{jk}$ and $\mathbf{B}_{jk}$ are orthogonal matrices and $\mathbf{D}_{jk}$ is a diagonal matrix. If σ_{jk} is proportional to an orthogonal matrix, then we can diagonalized it using only one matrix (instead of two as the singular value decomposition indicates), let us say $\mathbf{N}_j$, and use the other $\mathbf{N}_k$ in the diagonalization process of another $\sigma_{k,l}$ matrix (see Ref. [43] for details).

It has been shown also that, for a three-mode Gaussian state, the standard form is a covariance matrix with no Q-P correlations; that is, it has the form

$$\mathbf{\Sigma}^{(qp)} = \begin{pmatrix} \mathbf{\Sigma}^q & \mathbf{0} \\ \mathbf{0} & \mathbf{\Sigma}^p \end{pmatrix}, \tag{B1}$$

which, when written in the mode ordering, has the form

$$\mathbf{\Sigma} = \begin{pmatrix} \lambda_1 \mathbb{1} & \mathbf{D}_{1,2} & \mathbf{D}_{1,3} \\ & \lambda_2 \mathbb{1} & \mathbf{D}_{2,3} \\ & & \lambda_3 \mathbb{1} \end{pmatrix}, \tag{B2}$$

where $\mathbf{D}_{jk}$ are diagonal matrices and $\mathbb{1}$ is the 2×2 identity matrix. If we suppose that all three $\mathbf{D}_{jk}$ matrices have negative determinants, then we have

$$\mathbf{D}_{jk} = \begin{pmatrix} \alpha_{jk} & 0 \\ 0 & \beta_{jk} \end{pmatrix}, \quad \text{with} \quad \alpha_{jk}\beta_{jk} < 0, \tag{B3}$$

and we can transform the covariance matrix in (B2) into a covariance matrix with diagonal **U** (i.e., $\langle Q_j Q_k \rangle = 0\, j \neq k$) in two steps. We first apply the following local squeezing operations given by the GLUs:

$$\mathbf{S}_1^{(a)} = \begin{pmatrix} \sqrt{-\frac{\alpha_{1,2}}{\beta_{1,2}}} & 0 \\ 0 & \sqrt{-\frac{\beta_{1,2}}{\alpha_{1,2}}} \end{pmatrix},$$

$$\mathbf{S}_3^{(a)} = \begin{pmatrix} \sqrt{-\frac{\alpha_{1,3}}{\beta_{1,3}}} & 0 \\ 0 & \sqrt{-\frac{\beta_{1,3}}{\alpha_{1,3}}} \end{pmatrix}, \mathbf{S}_1^{(a)-1} \qquad \mathbf{S}_2^{(a)} = \mathbb{1}. \tag{B4}$$

This leads us to a covariance matrix of the form

$$\mathbf{\Sigma} = \begin{pmatrix} \lambda_1 \mathbf{S}_1^{(a)} \mathbf{S}_1^{(a)T} & \mp\sqrt{-\alpha_{1,2}\beta_{1,2}}\sigma_z & \mp\sqrt{-\alpha_{1,3}\beta_{1,3}}\sigma_z \\ & \lambda_2 \mathbb{1} & \mathbf{D}'_{2,3} \\ & & \lambda_3 \mathbf{S}_3^{(a)} \mathbf{S}_3^{(a)T} \end{pmatrix}, \tag{B5}$$

where the upper sign corresponds to $\alpha_{jk} < 0, \beta_{jk} > 0$ and the lower sign corresponds to the opposite situation, $\mathbf{D}'_{2,3} = \mathrm{diag}\{\alpha'_{2,3}, \beta'_{2,3}\} = \mathrm{diag}\{\alpha_{2,3}\sqrt{(\beta_{1,2}\alpha_{1,3}/\alpha_{1,2}\beta_{1,3})}, \beta_{2,3}\sqrt{(\alpha_{1,2}\beta_{1,3}/\beta_{1,2}\alpha_{1,3})}\}$, and $\sigma_z = \mathrm{diag}\{1, -1\}$ is one of the Pauli matrices. In the second step we apply the local rotations given by

$$\mathbf{S}_1^{(b)} = \mathbf{F}\mathbf{S}_2^{(b)T}, \qquad \mathbf{S}_3^{(b)} = \mathbf{F}\mathbf{S}_1^{(b)T} = \mathbf{S}_2^{(b)}, \tag{B6}$$

where $\mathbf{S}_2^{(b)}$ is a rotation to be determined later, $\mathbf{F} = \left(\begin{smallmatrix} 0 & 1 \\ -1 & 0 \end{smallmatrix}\right)$ is a $\pi/2$ rotation (also called the Fourier transform due to the way it act on quantum states), and use the fact that rotations in a plane commute with each other. Then given that

$$\sigma_z \mathbf{F}^T = \mathbf{F}\sigma_z = -\begin{pmatrix} 0 & 1 \\ 1 & 0 \end{pmatrix} \equiv -\mathbf{J} \quad \text{and} \quad \sigma_z \mathbf{M} = \mathbf{M}^T \sigma_z \tag{B7}$$

for any pure two-dimensional rotation matrix **M**, we have

$$\mathbf{\Sigma} = \begin{pmatrix} \lambda_1 \mathbf{S}_1 \mathbf{S}_1^T & \pm\sqrt{-\alpha_{1,2}\beta_{1,2}}\mathbf{J} & \pm\sqrt{-\alpha_{1,3}\beta_{1,3}}\mathbf{J} \\ & \lambda_2 \mathbf{S}_2 \mathbf{S}_2^T & \mathbf{S}_2^{(b)} \mathbf{D}'_{2,3} \mathbf{S}_2^{(b)T} \\ & & \lambda_3 \mathbf{S}_3 \mathbf{S}_3^T \end{pmatrix}, \tag{B8}$$

where $\mathbf{S}_j = \mathbf{S}_j^{(b)} \mathbf{S}_j^{(a)}$ is the total local transformation. The $\mathbf{S}_2^{(b)}$ matrix is set such that the Q-Q correlation $\langle Q_2 Q_3 \rangle = 0$ in the matrix $\mathbf{S}_2^{(b)} \mathbf{D}'_{2,3} \mathbf{S}_2^{(b)T}$. For that we write it as a generic two-dimensional rotation:

$$\mathbf{S}_2^{(b)} = \begin{pmatrix} \cos\theta & \sin\theta \\ -\sin\theta & \cos\theta \end{pmatrix}. \tag{B9}$$

Then the correlation matrix between modes 2 and 3 is

$$\mathbf{S}_2^{(b)} \mathbf{D}'_{2,3} \mathbf{S}_2^{(b)T} = \begin{pmatrix} \alpha'_{2,3}\cos^2\theta + \beta'_{2,3}\sin^2\theta & (\beta'_{2,3} - \alpha'_{2,3})\sin\theta\cos\theta \\ (\beta'_{2,3} - \alpha'_{2,3})\sin\theta\cos\theta & \alpha'_{2,3}\sin^2\theta + \beta'_{2,3}\cos^2\theta \end{pmatrix}. \tag{B10}$$

In the equation above, is possible to eliminate the Q-Q term (upper-left term in the matrix) only if $\alpha'_{2,3}$ and $\beta'_{2,3}$ have opposite sign; that is, if $\det\{\mathbf{D}'_{2,3}\} = \alpha'_{2,3}\beta'_{2,3} < 0$. In this case we can chose $\cos\theta = (\sqrt{-\beta_{2,3}}/\sqrt{\alpha_{2,3} - \beta_{2,3}})$, $\sin\theta =$

$(\sqrt{\alpha_{2,3}}/\sqrt{\alpha_{2,3}-\beta_{2,3}})$ for $\beta_{2,3}<0$ or $\cos\theta=(\sqrt{\beta_{2,3}}/\sqrt{\beta_{2,3}-\alpha_{2,3}})$, $\sin\theta=(\sqrt{-\alpha_{2,3}}/\sqrt{\beta_{2,3}-\alpha_{2,3}})$ for $\alpha_{2,3}<0$, and then

$$\mathbf{S}_2^{(b)}\mathbf{D}'_{2,3}\mathbf{S}_2^{(b)T}=\begin{pmatrix}0 & \pm\sqrt{-\alpha_{2,3}\beta_{2,3}}\\ \pm\sqrt{-\alpha_{2,3}\beta_{2,3}} & \alpha_{2,3}+\beta_{2,3}\end{pmatrix}, \tag{B11}$$

where the minus sign corresponds to $\alpha_{2,3}<0$ and the plus sign corresponds to $\beta_{2,3}<0$. In this way we have removed all the diagonal terms of $\mathbf{U}$.

In this procedure we first use single-mode squeezing operations to make the correlation matrices $\sigma_{1,2}$ and $\sigma_{1,3}$ proportional to the Pauli matrix σ_z, and use rotations to eliminate the Q-Q correlations [the first step is useful because using Eq. (B7), we can transform a given correlation matrix σ_{jk}, $j\neq k$, to a matrix proportional to $\mathbf{J}$ by using, let us say, $\mathbf{S}_j$ regardless of the value of $\mathbf{S}_k$].

This procedure is not enough for a general N-mode Gaussian state given that the number of correlation matrices $\sigma_{jk}, j\neq k$, is $N(N-1)/2$ and we have only N GLUs to eliminate all the Q-Q correlations, but for $N=3$ we have $N(N-1)/2=N$.

For $N>3$, the procedure can only be successful if the state exhibits a high enough degree of symmetry.

APPENDIX C: DETAILED U DIAGONALIZATION PROCEDURE

1. Negative-determinant correlation submatrices

If we start by operating in the matrix σ_{12}, then the explicit form of $\mathbf{S}_1$ [$\mathbf{S}_2$] is

$$\mathbf{S}_1[\mathbf{S}_2]=\begin{pmatrix}\frac{r_2}{\delta_{12}}\left(c_{12}\cos\phi_2-d_{12}\sin\phi_2\right) & \frac{r_2}{\delta_{12}}\left(b_{12}\sin\phi_2-a_{12}\cos\phi_2\right)\\ \frac{2\delta_{12}}{r_2}\frac{a_{12}\cos\phi_2-b_{12}\sin\phi_2}{\epsilon_{12}\sin 2\phi_2+\tau_{12}\cos 2\phi_2+\rho_{12}} & \frac{2\delta_{12}}{r_2}\frac{c_{12}\cos\phi_2-d_{12}\sin\phi_2}{\epsilon_{12}\sin 2\phi_2+\tau_{12}\cos 2\phi_2+\rho_{12}}\end{pmatrix}, \tag{C1}$$

where $\delta_{jk}=\sqrt{-\det[\sigma_{jk}]}=\sqrt{b_{jk}c_{jk}-a_{jk}d_{jk}}$ and

$$\epsilon_{12}=-2a_{12}b_{12}-2c_{12}d_{12}, \tag{C2}$$

$$\tau_{12}=a_{12}^2-b_{12}^2+c_{12}^2-d_{12}^2, \tag{C3}$$

$$\rho_{12}=a_{12}^2+b_{12}^2+c_{12}^2+d_{12}^2. \tag{C4}$$

Then we can move throughout the first block row of $\mathbf{\Sigma}^{(\mathrm{mode})}$, Eq. (35), and bring the correlations matrices σ_{1j} $j=3,4,\ldots,N$ to the desired form using the GLUs $\mathbf{S}_j$ $j=3,4,\ldots,N$ from the right as in Eq. (50) with $\mathbf{M}=\mathbf{S}_1\sigma_{1j}$. Similar to the case above, and given that $\mathbf{S}_1$ is now a function of $\mathbf{S}_2$, we end up with matrices $\mathbf{S}_j$ as functions of $\mathbf{S}_2$, $\mathbf{S}_j=\mathbf{S}_j[\mathbf{S}_2]$. Again, all the matrices σ_{1j} will be in the desired form regardless of the value of $\mathbf{S}_2$. Explicitly, the matrices $\mathbf{S}_j[\mathbf{S}_2]$ are

$$\mathbf{S}_j[\mathbf{S}_2]=\begin{pmatrix}\frac{r_2}{\delta_{12}\delta_{1j}}\left(\gamma_{1j}\sin\phi_2+\eta_{1j}\cos\phi_2\right) & \frac{r_2}{\delta_{12}\delta_{1j}}\left(\mu_{1j}\sin\phi_2+\nu_{1j}\cos\phi_2\right)\\ -\frac{\delta_{12}\delta_{1j}}{r_2}\frac{\mu_{1j}\sin\phi_2+\nu_{1j}\cos\phi_2}{\zeta_{1j}\sin 2\phi_2+\kappa_{1j}+\xi_{1j}\cos 2\phi_2} & \frac{\delta_{12}\delta_{1j}}{r_2}\frac{\gamma_{1j}\sin\phi_2+\eta_{1j}\cos\phi_2}{\zeta_{1j}\sin 2\phi_2+\kappa_{1j}+\xi_{1j}\cos 2\phi_2}\end{pmatrix}$$
$$\text{for all } j=3,4,\ldots,N, \tag{C5}$$

with

$$\kappa_{1j}=\frac{1}{2}\left[\left(c_{12}^2+d_{12}^2\right)\left(a_{1j}^2+b_{1j}^2\right)-2\left(a_{12}c_{12}+b_{12}d_{12}\right)\left(a_{1j}c_{1j}+b_{1j}d_{1j}\right)+\left(a_{12}^2+b_{12}^2\right)\left(c_{1j}^2+d_{1j}^2\right)\right], \tag{C6}$$

$$\zeta_{1j}=-c_{12}d_{12}\left(a_{1j}^2+b_{1j}^2\right)+\left(a_{12}d_{12}+b_{12}c_{12}\right)\left(a_{1j}c_{1j}+b_{1j}d_{1j}\right)-a_{12}b_{12}\left(c_{1j}^2+d_{1j}^2\right), \tag{C7}$$

$$\xi_{1j}=\frac{1}{2}\left[\left(c_{12}^2-d_{12}^2\right)\left(a_{1j}^2+b_{1j}^2\right)+2\left(b_{12}d_{12}-a_{12}c_{12}\right)\left(a_{1j}c_{1j}+b_{1j}d_{1j}\right)+\left(a_{12}^2-b_{12}^2\right)\left(c_{1j}^2+d_{1j}^2\right)\right], \tag{C8}$$

$$\gamma_{1j} = b_{12}d_{1j} - d_{12}b_{1j}, \tag{C9}$$

$$\eta_{1j} = c_{12}b_{1j} - a_{12}d_{1j}, \tag{C10}$$

$$\mu_{1j} = d_{12}a_{1j} - b_{12}c_{1j}, \tag{C11}$$

$$\nu_{1j} = a_{12}c_{1j} - c_{12}a_{1j}. \tag{C12}$$

Once this procedure is complete, we have all elements $\mathbf{U}_{1j} = 0, j = 2, 3, \ldots, N$, so now all the edges connecting qumode 1 with the rest of the graph can only be real. So far, we have set $N-1$ of the GLUs. For the last one we just take any other of the remaining correlation matrices to the desired form, Eq. (40), let us say the matrix σ_{23}:

$$\sigma'_{23} = \mathbf{S}_2\sigma_{23}\mathbf{S}_3\,[\mathbf{S}_2]^T. \tag{C13}$$

It is of course enough to set the upper-left element to zero. This has the form

$$a'_{23} = r_2\,(A\cos 2\phi_2 + B\sin 2\phi_2 + C), \tag{C14}$$

and $a'_{2,3} = 0$ has real solutions (two) for ϕ_2 if and only $C^2 \leq A^2 + B^2$. Again, which solution is the correct one will be determined by testing the solutions on the remaining correlation submatrices.

2. Singular correlation submatrices

The case $\sigma_{j,k} = 0$, does not give us any information about the required GLUs $\mathbf{S}_j$ and $\mathbf{S}_k$, so we just move to the next nonzero submatrix. If $\sigma_{j,k} \neq 0$ then, defining $\mathbf{M} = \left(\begin{smallmatrix} a & b \\ c & d \end{smallmatrix}\right) = \sigma_{jk}\mathbf{S}_{\text{right}}^T$ a general 2×2 matrix with null determinant. Then we can operate with a sympletic matrix to the left such that the upper-right component of the correlation submatrix will be set to zero ($\det[\sigma_{j,k}] = 0$ also means that the off-diagonal terms of $\sigma_{j\neq k}$ are also zero), i.e.,

$$\mathbf{S}_{\text{left}}\mathbf{M} = \begin{pmatrix} 0 & 0 \\ \frac{ab+cd}{r\sqrt{b^2+d^2}} & \frac{\sqrt{b^2+d^2}}{r} \end{pmatrix}, \tag{C15}$$

where the upper-left component is automatically zero too because $\det[\mathbf{M}] = ad - bc = 0$. To achieve this we set the rotation

$$\cos\phi_{\text{left}} = \frac{d}{\sqrt{b^2+d^2}}, \tag{C16}$$

$$\sin\phi_{\text{left}} = \frac{b}{\sqrt{b^2+d^2}}, \tag{C17}$$

and the squeezing parameter r_{left} remains to be determined later in the algorithm. If $\mathbf{S}_{\text{right}}$ was already defined in a previous step of the algorithm, then the lower-left term in Eq. (C15) must be also zero, otherwise it means that the state is not GLU-equivalent to a cluster state. In the case that $\mathbf{S}_{\text{right}}$ was not determined yet, we can use it to impose $ab + cd = 0$. This is easily done by setting ϕ_{right} such that

$$\cos 2\phi_{\text{right}} = \frac{a_{jk}^2 - b_{jk}^2 + c_{jk}^2 - d_{jk}^2}{N_{jk}}, \tag{C18}$$

$$\sin 2\phi_{\text{right}} = \frac{-2\left(a_{jk}b_{jk} + c_{jk}d_{jk}\right)}{N_{jk}}, \tag{C19}$$

$$N_{jk} = \sqrt{4\left(a_{jk}b_{jk} + c_{jk}d_{jk}\right)^2 + \left(a_{jk}^2 - b_{jk}^2 + c_{jk}^2 - d_{jk}^2\right)^2}, \tag{C20}$$

where, as before, the squeezing parameter r_{right} can be used in another stage of the algorithm. It is worth pointing out that in this case, where $\det[\sigma_{jk}] = 0$, we need both ϕ_{left} and ϕ_{right} to take σ_{jk} to the standard form, in contrast to the case $\det[\sigma_{j,k}] \neq 0$ as we saw above. There are two different solutions to Eq. (C18) (if a given ϕ is a solution, then $\phi + \pi$ is also a solution corresponding to a different rotation), but which one has to be picked will be determined by applying both solutions in following steps on the algorithm.

[1] S. L. Braunstein and P. van Loock, Quantum information with continuous variables, Rev. Mod. Phys. **77**, 513 (2005).

[2] C. Weedbrook, S. Pirandola, R. García-Patrón, N. J. Cerf, T. C. Ralph, J. H. Shapiro, and S. Lloyd, Gaussian quantum information, Rev. Mod. Phys. **84**, 621 (2012).

[3] O. Pfister, Continuous-variable quantum computing in the quantum optical frequency comb, J. Phys. B: At. Mol. Opt. Phys. **53**, 012001 (2019).

[4] M. Pysher, Y. Miwa, R. Shahrokhshahi, R. Bloomer, and O. Pfister, Parallel Generation of Quadripartite Cluster Entanglement in the Optical Frequency Comb, Phys. Rev. Lett. **107**, 030505 (2011).

[5] M. Chen, N. C. Menicucci, and O. Pfister, Experimental Realization of Multipartite Entanglement of 60 Modes of a Quantum Optical Frequency Comb, Phys. Rev. Lett. **112**, 120505 (2014).

[6] S. Yokoyama, R. Ukai, S. C. Armstrong, C. Sornphiphatphong, T. Kaji, S. Suzuki, J. Yoshikawa, H. Yonezawa, N. C. Menicucci, and A. Furusawa, Ultra-large-scale continuous-variable cluster states multiplexed in the time domain, Nat. Photon. **7**, 982 (2013).

[7] J.-i. Yoshikawa, S. Yokoyama, T. Kaji, C. Sornphiphatphong, Y. Shiozawa, K. Makino, and A. Furusawa, Invited article: Generation of one-million-mode continuous-variable cluster state by unlimited time-domain multiplexing, APL Photonics **1**, 060801 (2016).

[8] W. Asavanant *et al.*, Generation of time-domain-multiplexed two-dimensional cluster state, Science **366**, 373 (2019).

[9] M. V. Larsen, X. Guo, C. R. Breum, J. S. Neergaard-Nielsen, and U. L. Andersen, Deterministic generation of a two-dimensional cluster state, Science **366**, 369 (2019).

[10] N. C. Menicucci, P. van Loock, M. Gu, C. Weedbrook, T. C. Ralph, and M. A. Nielsen, Universal Quantum Computation with Continuous-Variable Cluster States, Phys. Rev. Lett. **97**, 110501 (2006).

[11] J. Zhang and S. L. Braunstein, Continuous-variable Gaussian analog of cluster states, Phys. Rev. A **73**, 032318 (2006).

[12] S. Lloyd and S. L. Braunstein, Quantum Computation Over Continuous Variables, Phys. Rev. Lett. **82**, 1784 (1999).

[13] D. Gottesman, A. Kitaev, and J. Preskill, Encoding a qubit in an oscillator, Phys. Rev. A **64**, 012310 (2001).

[14] S. D. Bartlett, B. C. Sanders, S. L. Braunstein, and K. Nemoto, Efficient Classical Simulation of Continuous Variable Quantum Information Processes, Phys. Rev. Lett. **88**, 097904 (2002).

[15] A. Mari and J. Eisert, Positive Wigner Functions Render Classical Simulation of Quantum Computation Efficient, Phys. Rev. Lett. **109**, 230503 (2012).

[16] N. C. Menicucci, Fault-Tolerant Measurement-Based Quantum Computing with Continuous-Variable Cluster States, Phys. Rev. Lett. **112**, 120504 (2014).

[17] K. Fukui, A. Tomita, A. Okamoto, and K. Fujii, High-Threshold Fault-Tolerant Quantum Computation with Analog Quantum Error Correction, Phys. Rev. X **8**, 021054 (2018).

[18] B. W. Walshe, L. J. Mensen, B. Q. Baragiola, and N. C. Menicucci, Robust fault tolerance for continuous-variable cluster states with excess antisqueezing, Phys. Rev. A **100**, 010301 (2019).

[19] H. Vahlbruch, M. Mehmet, K. Danzmann, and R. Schnabel, Detection of 15 dB Squeezed States of Light and Their Application for the Absolute Calibration of Photoelectric Quantum Efficiency, Phys. Rev. Lett. **117**, 110801 (2016).

[20] N. C. Menicucci, S. T. Flammia, and P. van Loock, Graphical calculus for Gaussian pure states, Phys. Rev. A **83**, 042335 (2011).

[21] Recall that controlled-Z gates define the edges of qubit-vertex graph states, also known as cluster states [25], which enable measurement-based one-way quantum computing [27].

[22] M. Gu, C. Weedbrook, N. C. Menicucci, T. C. Ralph, and P. van Loock, Quantum computing with continuous-variable clusters, Phys. Rev. A **79**, 062318 (2009).

[23] In contrast, the graph defined by the imaginary edges cannot be used for measurement-based quantum computing as that would require measuring non-Hermitian observables.

[24] GLUs are operations generated by all single-mode phase-space rotations (i.e., optical phase shifts), single-mode squeezes, and single-mode shears (which are combinations of the former two). GLUs are equivalent to single-mode symplectic operations because $\mathrm{Sp}(2,\mathbb{R}) \sim \mathrm{SU}(1,1) \supset \mathrm{U}(1)$.

[25] H. J. Briegel and R. Raussendorf, Persistent Entanglement in Arrays of Interacting Particles, Phys. Rev. Lett. **86**, 910 (2001).

[26] M. Hein, J. Eisert, and H. J. Briegel, Multiparty entanglement in graph states, Phys. Rev. A **69**, 062311 (2004).

[27] R. Raussendorf and H. J. Briegel, A One-Way Quantum Computer, Phys. Rev. Lett. **86**, 5188 (2001).

[28] D. Bacon, Too entangled to quantum compute one-way, Physics **2**, 38 (2009).

[29] D. Gross, S. T. Flammia, and J. Eisert, Most Quantum States are too Entangled to be Useful as Computational Resources, Phys. Rev. Lett. **102**, 190501 (2009).

[30] M. J. Bremner, C. Mora, and A. Winter, Are Random Pure States Useful for Quantum Computation?, Phys. Rev. Lett. **102**, 190502 (2009).

[31] Weighted real graphs also appear in qudit graph state theory but complex graphs are a property of CV systems.

[32] Without loss of generality, we consider only states with $\langle P_j \rangle = \langle Q_j \rangle = 0$ since that does not affect the entanglement properties of the system.

[33] X. Zhu, C.-H. Chang, C. González-Arciniegas, A. Pe'er, J. Higgins, and O. Pfister, Hypercubic cluster states in the phase-modulated quantum optical frequency comb, Optica **8**, 281 (2021).

[34] R. Bruckmeier, H. Hansen, S. Schiller, and J. Mlynek, Realization of a Paradigm for Quantum Measurements: The Squeezed Light Beam Splitter, Phys. Rev. Lett. **79**, 43 (1997).

[35] A. Peres, Separability Criterion for Density Matrices, Phys. Rev. Lett. **77**, 1413 (1996).

[36] M. Horodecki, P. Horodecki, and R. Horodecki, Separability of mixed states: Necessary and sufficient conditions, Phys. Lett. A **223**, 1 (1996).

[37] R. Simon, Peres-Horodecki Separability Criterion for Continuous Variable Systems, Phys. Rev. Lett. **84**, 2726 (2000).

[38] L.-M. Duan, G. Giedke, J. Cirac, and P. Zoller, Inseparability Criterion for Continuous Variable Systems, Phys. Rev. Lett. **84**, 2722 (2000).

[39] G. Adesso, Generic Entanglement and Standard Form for N-Mode Pure Gaussian States, Phys. Rev. Lett. **97**, 130502 (2006).

[40] Z. Y. Ou, S. F. Pereira, H. J. Kimble, and K. C. Peng, Realization of the Einstein-Podolsky-Rosen Paradox for Continuous Variables, Phys. Rev. Lett. **68**, 3663 (1992).

[41] A. Furusawa, J. L. Sørensen, S. L. Braunstein, C. A. Fuchs, H. J. Kimble, and E. S. Polzik, Unconditional quantum teleportation, Science **282**, 706 (1998).

[42] This doe snot detract from the generality of our approach because any $\mathbf{V}_{jj} \neq 0$ can be removed via GLU $\mathbf{S}_j = \begin{pmatrix} 1 & 0 \\ -\mathbf{V}_{jj} & 1 \end{pmatrix}$.

[43] G. Giedke and B. Kraus, Gaussian local unitary equivalence of n-mode Gaussian states and Gaussian transformations by local operations with classical communication, Phys. Rev. A **89**, 012335 (2014).

[44] Arvind, B. Dutta, N. Mukunda, and R. Simon, Two-mode quantum systems: Invariant classification of squeezing transformations and squeezed states, Phys. Rev. A **52**, 1609 (1995).

[45] R. Simon, E. C. G. Sudarshan, and N. Mukunda, Gaussian pure states in quantum mechanics and the symplectic group, Phys. Rev. A **37**, 3028 (1988).

[46] Arvind, B. Dutta, N. Mukunda, and R. Simon, The real symplectic groups in quantum mechanics and optics, Pramana J. Phys. **45**, 471 (1995).

[47] G. Adesso and F. Illuminati, Continuous variable tangle, monogamy inequality, and entanglement sharing in

Gaussian states of continuous variable systems, New J. Phys. **8**, 15 (2006).

[48] S. L. Braunstein, Squeezing as an irreducible resource, Phys. Rev. A **71**, 055801 (2005).

[49] C. S. Hamilton, R. Kruse, L. Sansoni, S. Barkhofen, C. Silberhorn, and I. Jex, Gaussian Boson Sampling, Phys. Rev. Lett. **119**, 170501 (2017).

[50] A. Einstein, B. Podolsky, and N. Rosen, Can quantum-mechanical description of physical reality be considered complete?, Phys. Rev. **47**, 777 (1935).

[51] M. Reid, Demonstration of the einstein-podolsky-Rosen paradox using nondegenerate parametric amplification, Phys. Rev. A **40**, 913 (1989).

[52] M. Kim, W. Son, V. Bužek, and P. Knight, Entanglement by a beam splitter: Nonclassicality as a prerequisite for entanglement, Phys. Rev. A **65**, 032323 (2002).

[53] For any n-mode CV with no p-q correlations, the extrema of Tr[U] after local rotations are located at a rotation angle of $\pi/2$ of any subset of the original n modes [20].